

CENTRE FOR
AUTOMOTIVE
SAFETY RESEARCH



THE UNIVERSITY
of ADELAIDE

Impact characteristics of the New Zealand Fisheries sea lion exclusion device stainless steel grid

G Ponte, A van den Berg, RWG Anderson

Final Research Report for Ministry of Fisheries project IPA2009-06

October 2010

Report documentation

DATE

October 2010

PAGES

19

TITLE

Impact characteristics of the New Zealand Fisheries sea lion exclusion device stainless steel grid: Final Research Report for Ministry of Fisheries project IPA2009-06

AUTHORS

G Ponte, A van den Berg, RWG Anderson

PERFORMING ORGANISATION

Centre for Automotive Safety Research
The University of Adelaide
South Australia 5005
AUSTRALIA

SPONSORED BY

Ministry of Fisheries
PO Box 1020
Wellington

AVAILABLE FROM

Centre for Automotive Safety Research
<http://casr.adelaide.edu.au/publications/researchreports>

KEYWORDS

Sea Lion Exclusion Device, Impact Testing, Head Injury

Summary

This report documents the instrumentation, test methods, results and analysis used to assess the likelihood of brain injury to a sea lion as a result of a head impact with a sea lion exclusion device (SLED) stainless steel grid. The testing used a validated method for measuring head impact injury in human pedestrians and was then subsequently scaled and extrapolated with consideration of the head and brain mass of the New Zealand sea lion.

The results of the tests are used as the basis of a graphical method for determining a range of the likelihood of a brain injury, based on swim speed and effective sea lion head mass, for particular impact locations.

The results indicate that an impact with the grid may induce some sort of brain injury in sea lions; the risk of life-threatening brain injury to a female sea lion in a 10 m/s collision with the SLED grid at the stiffest location tested may be higher than 85%.

Although some assumptions were made to arrive at the results, this report provides base-line results for the impact characteristics for the current grid design. This will allow a baseline for the assessment of future grid modifications.

Contents

- 1 Introduction1
- 2 Background2
 - 2.1 Head injury assessment2
 - 2.2 Dependence of Head Injury Criterion values on impact speed and impact mass2
 - 2.3 Estimation of sea lion head injury risk based on human head risk3
- 3 Test methods8
 - 3.1 Test Locations8
 - 3.2 Test matrix9
- 4 Results11
 - 4.1 Locations 1 and 211
 - 4.2 Location 315
 - 4.3 Verification of scaling method16
- 5 Discussion and Recommendations17
 - 5.1 SLED grid design17
- 6 Acknowledgements19
- 7 References20
- 8 Appendices22

1 Introduction

Sea lion exclusion devices (SLEDs) have been used extensively since 2004-05 as a central strategy in the management of the by-catch of New Zealand sea lions (*Phocarctos hookeri*). However, the effectiveness of SLEDs in reducing mortality remains uncertain.

The SLED consists of a stainless steel grid and an escape hatch, located near the cod end of a trawler net (Figure 1). The intention is that, during a trawl, fish or squid pass through the grid undamaged into the cod end of the trawler nets, while the grid diverts sea lions toward the escape hatch.

Prior to SLED use, sea lions incidentally killed by fishing were generally retained in trawl nets and hauled on board, allowing observers to gain an accurate assessment of the number of sea lions dying in the fishery. However, following the introduction of SLEDs, the number of sea lions interacting with SLED grids, the extent of any injuries, and the proportion of those killed or surviving interactions with the SLED grid and net are not known. Anecdote and reports on similar devices used in Australian waters indicate that sea lions may make very heavy contact with the SLED grids (Lyle and Wilcox, 2008). Whether such contacts result in injury is currently unknown.

While the fact of such injuries remains somewhat controversial, it is possible to make an assessment of the severity of impacts that might occur upon heavy interaction between the head of a sea lion and the SLED grid. This report documents a series of impact tests with a SLED grid, and through extrapolation from what is known about human head injury tolerance, a reasoned estimate of injury risk is presented. Uncertainties in relation to impact speed, impact angle, effective head mass and impact tolerance have been accommodated in the interpretation of the results.

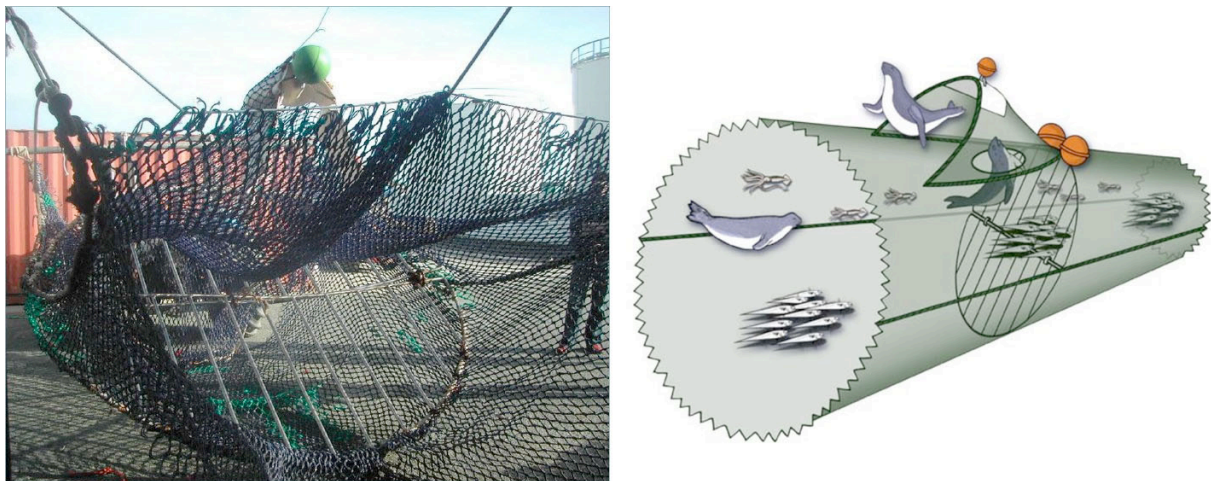


Figure 1

A photograph of a SLED (courtesy Dr Wendi Roe), and a diagram of the SLED, demonstrating the intended method of sea lion diversion (Tilzey and Wise, 2005)

2 Background

The methodology in this study uses impact tests to characterise the impact response of the SLED grid. The results are used as a basis for examining the likelihood of injury to the sea lion in an interaction with the grid, given the uncertainties that exist with respect to the reality of such interactions. In effect, the method is designed to assess whether such an injury is probable or indeed possible given the impact test results.

2.1 Head injury assessment

In vehicle crash testing, head impact severity is assessed using the deceleration of the head of a crash test dummy over the duration of the impact. The assessment takes account of the fact that the head appears to be more tolerant to high levels of deceleration if the impact duration is short, and less tolerant to deceleration when the duration is long.

This phenomenon is encapsulated in the function for injury assessment, the Head Injury Criterion (HIC). The Head Injury Criterion is calculated according to the formula

$$HIC = (t_2 - t_1) \left[\frac{\int_{t_1}^{t_2} a dt}{t_2 - t_1} \right]^{2.5}$$

where t is the time measured in milliseconds over impact duration, and a is the acceleration measured in units of g (the constant for acceleration due to gravity, i.e. 1 g is equivalent to 9.81 m/s/s). By definition, the values of t_2 and t_1 are set (by a mathematical algorithm) to maximise the HIC result. The difference between t_2 and t_1 is referred to as the HIC window. Impacts that produce HIC values of more than 1000 are considered to be unacceptably severe.

There are two main issues that we have considered in transferring accepted practice in human head injury assessment to assessment in the case of a sea lion. These are the difference in HIC values between the results of the impact tests and those probable in actual interactions (being due to differences in head mass and swim speed), and estimated differences in the impact tolerance of the sea lion and the human.

2.2 Dependence of Head Injury Criterion values on impact speed and impact mass

The value of HIC depends on several impact parameters: the stiffness of the object being struck, the mass of the headform (the dummy head) and the speed at which the impact takes place. HIC values with spring-like structures theoretically scale with speed raised to the power of 2.5, and with mass to the power of -0.75 (Searson and Anderson, 2008). These values have been confirmed from back-to-back testing on automotive structures. HIC values can be scaled to account for different head masses and velocities according to the following equation:

$$\frac{HIC_1}{HIC_2} = \left(\frac{m_1}{m_2} \right)^{-3/4} \left(\frac{v_1}{v_2} \right)^{5/2} \quad \text{Equation 1}$$

Where HIC_1 is the HIC value scaled to the impact conditions mass = m_1 and speed = v_1 from HIC_2 , being the result from an impact test, conducted with a headform impactor with a mass m_2 at an impact velocity v_2 . Searson and Anderson (2008) derived and validated Equation 1 by conducting a number of impact tests at identical locations on a car bonnet using varying impact speeds and varying headform impactor masses.

In the testing of the SLED, a headform weighing 4.8 kg was launched at maximum nominal impact speed of 10 m/s. In the case of a sea lion impact, there are uncertainties about effective impact speeds and the effective head mass during the interaction. But, using Equation 1, the test results can be scaled to estimate impact severity for different effective mass and speed combinations.

The headform mass selected (4.8 kg) is consistent with the mass of the head in adult female sea lions. Mass data was provided by Dr. Wendi Roe and Baukje Lenting, Massey University Institute of Veterinary, Animal, and Biomedical Sciences. This data showed the range of head masses is about 4.2-6.3 kg ($n=5$). The effective head mass in an impact may vary due to anatomical differences, and also because the weight of the body behind the head may contribute to the apparent mass of the head during the impact, through forces transmitted by the neck.

The speed of the test was based on the maximum (burst) swim speeds reported by Ray (1963) and Fish (2002) (via personal communication with Dr Eric Mellina, Aquatic Fisheries, New Zealand Ministry of Fisheries).

2.3 Estimation of sea lion head injury risk based on human head risk

Having explained the method for scaling the HIC results, we turn now to the issue of the risk of injury.

Figure 2 is the risk curve for life-threatening head injury in humans derived from Mertz (1993). According to this figure (see also Table 4 in the appendices), a HIC of 1000 corresponds to a 16% risk of life-threatening brain injury. For the purposes of assessing head impact injury in humans, and for vehicle design, the aim is to design structures that, when struck, produce a HIC below 1000.

Two things need to be considered in the current context. First, it is known that brain injury tolerance is related to brain mass and so some adjustment to accepted thresholds should be considered. Second, it may not be appropriate to consider a threshold value for HIC in this instance (e.g. HIC = 1000) but to consider the entire tolerance curve.

FATAL HEAD INJURY RISK

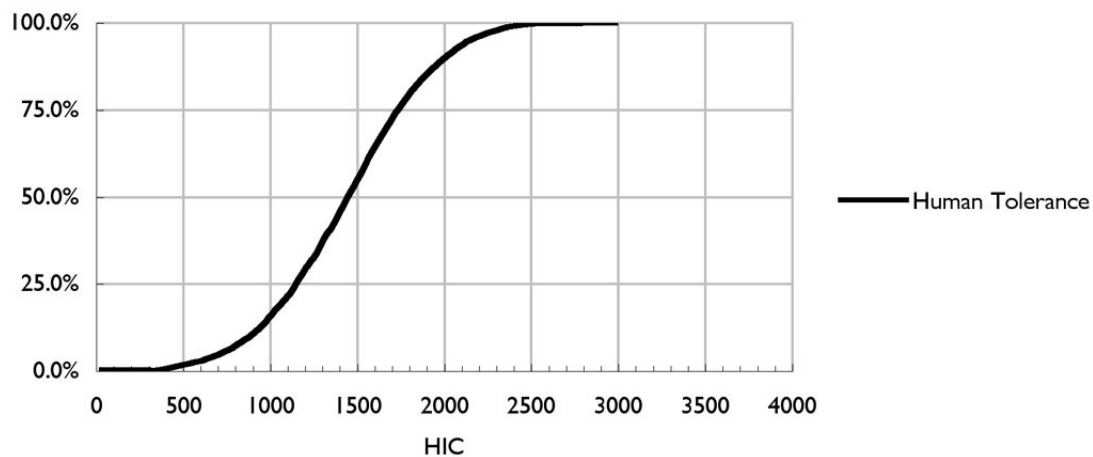


Figure 2
Injury risk curve for life-threatening brain injury risk (adapted from Mertz 1993)

As mentioned, the curve in Figure 2 cannot be used unaltered to describe the risk of fatal head injury to the New Zealand sea lion. There is reason to believe that the sea lion may be more tolerant to impact forces. A smaller brain mass tends to tolerate higher levels of deceleration and we are advised that the skull of the animal is thicker than that of a human skull. Anecdotal evidence also suggests that combative behaviour amongst male (but not female) sea lions has indicated considerable head strength and injury tolerance. The question is how much more tolerant the sea lion is to head impact.

At this point, it should be noted that HIC is based entirely on the linear acceleration of the head. However, a generally accepted theory is that the brain is also sensitive to angular accelerations induced by an impact (Gennarelli et al., 1982). But as the test tools only allow us to measure linear acceleration, and it is from this that we are able to derive HIC, for the purposes of this investigation it shall be assumed that the HIC values produced can be considered a proxy measure for both linear and angular mechanisms of injury.

Theoretical considerations and experimental data show that the ratio of impact tolerance is proportional to the inverse ratio of brain mass raised to some power. In the case of linear acceleration the power is 1/3 and for angular acceleration it is 2/3 (Goldsmith and Plunkett, 2004). This relationship is shown Figure 3. The line on the graph indicates the angular acceleration associated with a greater than 99% probability of concussion on various species of animals as a function of brain mass, and is based on tests performed on rhesus monkeys.

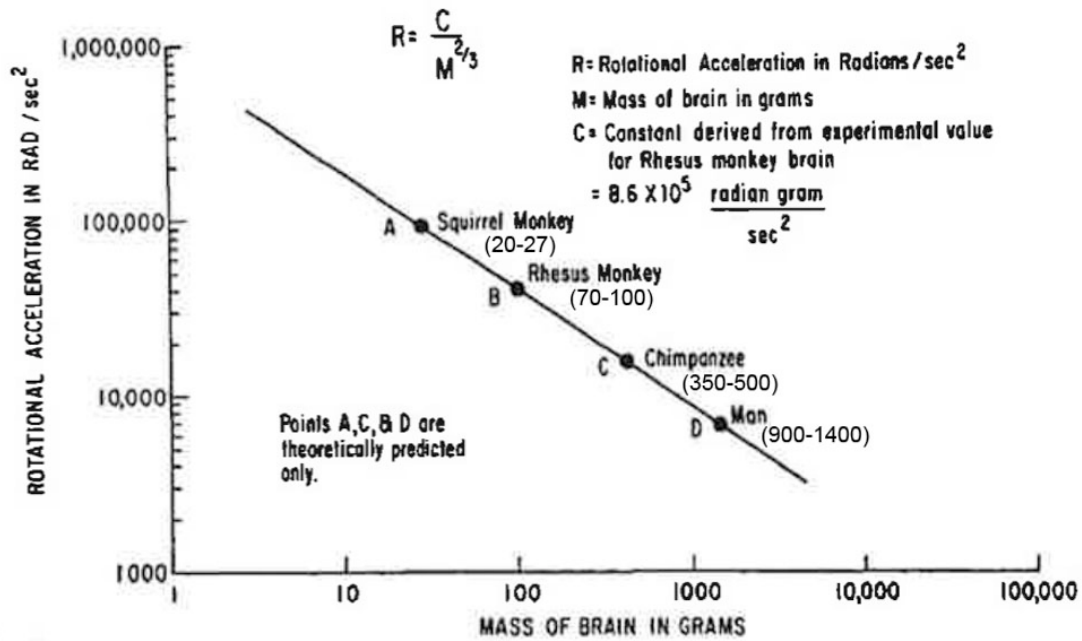


Figure 3
Theoretical concussion tolerance (>99% probability of concussion) as a function of angular acceleration and brain mass (Ommaya et al 1967, with brain mass ranges from Goldsmith and Plunkett, 2004)

The HIC at which an impact exceeds a sea lion’s tolerance need not be set too firmly, and results will be presented later that allow a range of levels to be considered in the interpretation of the test results.

The ratio of brain masses between human and sea lion suggest that the tolerance curve in Figure 2 might be scaled to the right: although there may be other reasons for differences in injury tolerance, here 1/3 and 2/3 power relationships will be used to scale the risk curve, consistent with other inter-species differences in head injury risk and as indicated in Figure 3. The predicted HIC curves for risk of fatal head injury to sea lions were adjusted according to Equation 1 where HIC_{human} is the impact test result based on the human headform, $n=1/3$ for linear acceleration tolerance, and $n=2/3$ for angular acceleration tolerance.

$$HIC_{sea_lion} = \left(\frac{m_{sea_lion_brain}}{m_{human_brain}} \right)^n \times HIC_{human} \quad (1)$$

Figure 4 illustrates this modification of the human fatal head injury risk curves with consideration of theorised injury tolerance in the sea lion. Here human brain mass is assumed to be 1360 grams and sea lion brain mass 500 grams. Table 4 (Appendix) also shows the theoretical HIC and corresponding fatal head injury that was derived from Mertz and scaled for sea lion impacts.

FATAL HEAD INJURY RISK

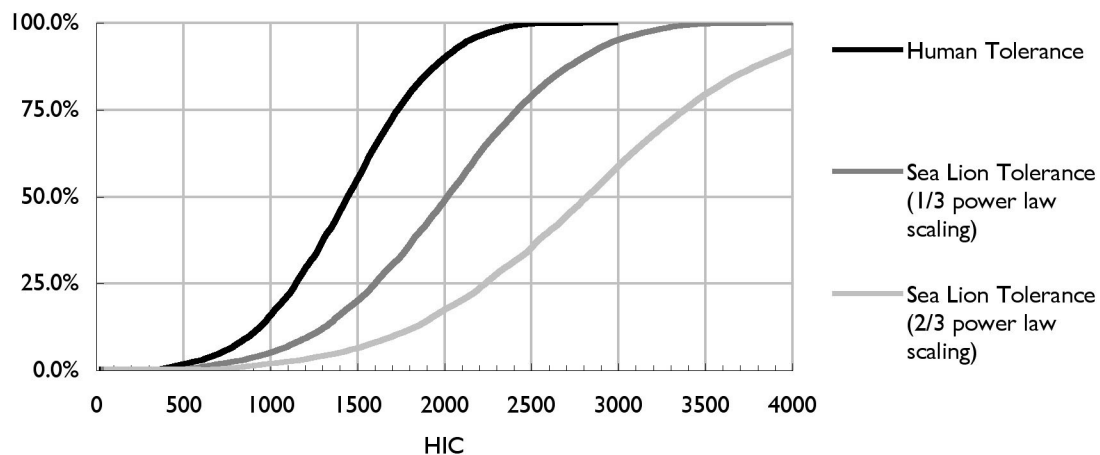


Figure 4
Fatal injury risk curves (derived from Mertz, 1993)

Not all head impacts will result in fatal head injuries, but the effects of moderate or mild impacts that may result in mild traumatic brain injury still need to be considered. Previously, one of our laboratory staff members struck a suspended adult headform with as much force as he could with a dead-blow hammer and the resulting HIC was around 650. There would be no doubt that a strike of that nature on a living animal or human would likely result in some sort of injury.

There is a limit to how long sea lions can remain submerged before needing to resurface for air. Any impediments to their ability to resurface may result in drowning. Lyle and Wilcox (2008) documented the duration of fur seal dives – the maximum was 14.8 minutes. They also refer to the physiological effects of increasing underwater exposure: lethargy and decreased responsiveness. With regard to seal interactions with seal excluder devices (SEDs), they conclude that a timely exit was important for survival; they write “...even if marine mammals can be directed out of the trawl gear, survival cannot be guaranteed”. Given that normal interactions with trawl gear and SLED may threaten a sea lion’s survival, any substantial physical contact between the sea lion and the grid may further threaten the safety of that sea lion through physiological impairment and subsequent drowning.

The effect of moderate or mild head impacts and their relationship to concussive head injury has been examined by Funk et al, (2007). They constructed various curves relating HIC to risk of mild traumatic brain injury. One such curve using their corrected experimental data is shown below in Figure 5.

RISK OF MILD TRAUMATIC BRAIN INJURY

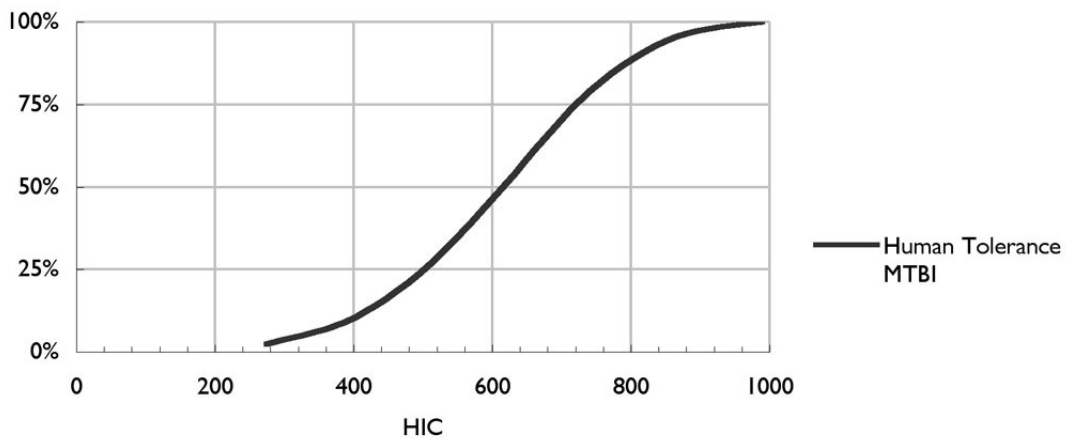


Figure 5
Injury risk curve for mild traumatic brain injury (adapted from Funk et al 2007)

Figure 5 shows that for a HIC of 1000 that there is almost 100% chance of mild traumatic brain injury in humans.

Using the scaling methods discussed above, risk curves for MTBI in the sea lions were derived and are presented in Figure 6. The data derived for generating this can be found in Table 5. Note that the MTBI referred to by these risk curves is enough to affect normal psycho-motor function in humans, and the relevance of this effect to an ability of a seal lion to successfully negotiate a SLED is not known.

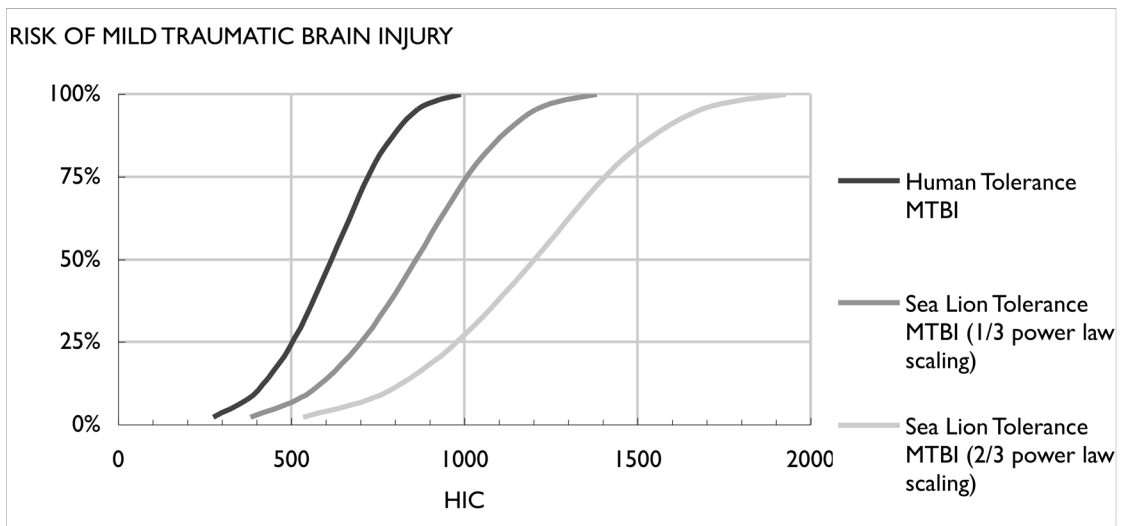


Figure 6
Mild traumatic brain Injury risk curves (derived from Funk et al (2007) and corresponding scaled tolerance curves for the sea lion based on 1/3 and 2/3 power relationships with brain mass.

3 Test methods

The testing of the grid was conducted using a 4.8 kg adult headform developed by the European Enhance Vehicle-Safety Committee Working Group 17 (EEVC WG17). The headform was designed for the assessment of pedestrian head protection. This headform consists of a truncated sphere of aluminium with a diameter of 165 mm. The sphere is covered with a 14 mm polyvinyl chloride skin to simulate the compliance of the scalp and bone of a human head. An aluminium base plate contains three accelerometers to measure the acceleration of the headform on impact. The headform and schematic is illustrated in Figure 7.

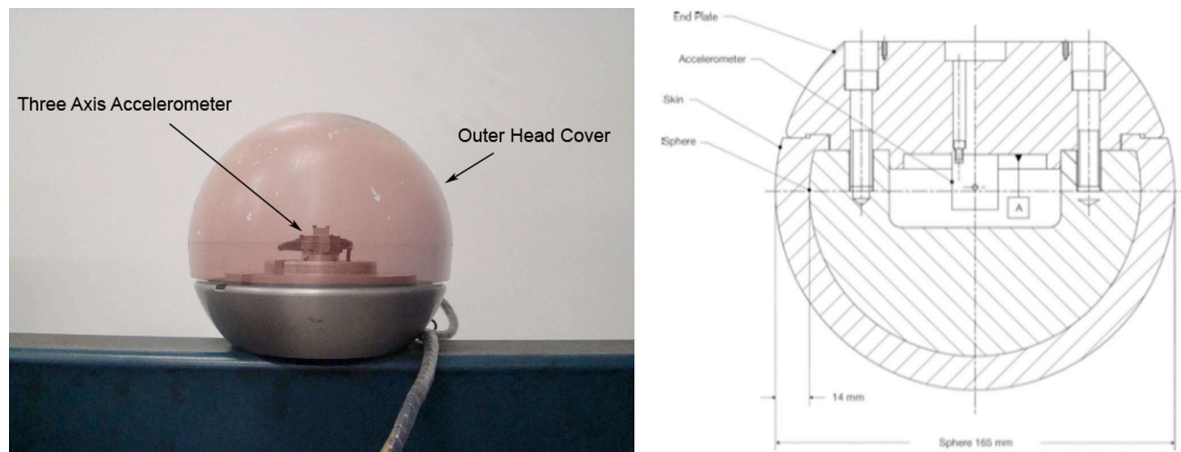


Figure 7
The 4.8 kg, 165 mm diameter adult pedestrian headform impactor and schematic

The SLED grid was held rigidly at various edge locations, and the test temperature was between 19 and 21° C. The headform was either suspended above the grid and dropped from a predetermined height (using the potential energy at a the height to generate the desired impact speed) or fired at the test location using a headform launching machine, and the speed measured.

The resulting impact acceleration was recorded using a high-speed data acquisition system (50 kHz) and then filtered according to SAE CFC1000 (SAE J211 MAR95 - Instrumentation for Impact Test - Part 1 - Electronic Instrumentation), and the Head Injury Criterion (HIC) was calculated.

3.1 Test Locations

Three locations were tested; these are illustrated in Figure 8. Location 1 was considered to be 'softer' and location 2 was considered to be 'hard' based on inspection. Locations 1 and 2 were struck at 90 degrees to the grid plane. For tests on location 3 the grid was rotated about the horizontal bottom bar so the impact angle could be varied between 90 degrees and 30 degrees to the grid plane. The objective of the tests on location 3 was to examine the effect of the swim approach angle on the severity of the impact.

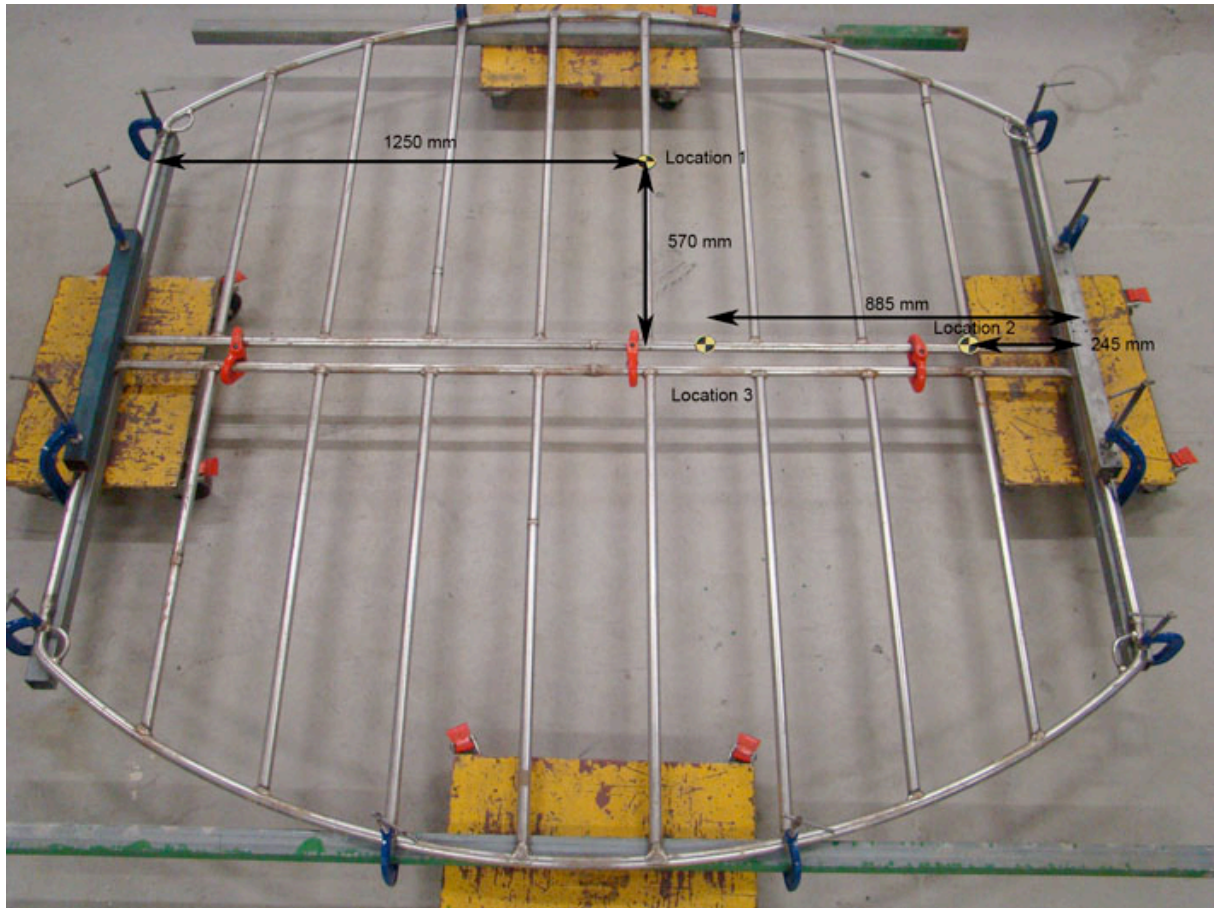


Figure 8
Assembled SLED grid with test locations indicated

3.2 Test matrix

Sixteen tests were conducted in total. Initially, some low speed drop tests (5 m/s) were conducted to evaluate the likelihood of instrumentation damage as well as looking at the effect of various boundary conditions (the manner in which the edge of the grid was constrained). These tests are not documented in the report. (The list of tests used in this report are given in Table 1.) The impact speed reflects the relative speed between the grid during a trawl (2 m/s) and the maximum swim speed of a sea lion (8 m/s).

We are not aware how rigidly the edge of the grid is maintained during a trawl. Therefore the boundary conditions represent an assumption about how the grid might behave in underwater operation. We have assumed that tension in the net would create quite rigid boundary conditions. According to the 2010 SLED Specifications (SLED WG, 2009) two halves of the grid are required to be “hinged horizontally along the middle”. It is possible that different trawlers may use different linking mechanisms between the two halves; in this report the tests conducted used hammerlocks as the hinging mechanism, which created a 56 mm gap between the two halves. Other SLED grids in operation may not use this mechanism and so it is possible that the mid section bar may be doubled-up along the centre line in some installations, such as the one shown in Figure 1.

At location 2, tests were conducted at different speeds to check the assumed relationship between HIC and impact speed used to generalise the results to other impact conditions.

Table 1
Test conditions

| Location | Test number | Nominal speed (m/s) | Boundary conditions |
|----------|-------------|---------------------|--|
| 1 | 13071000 | 10 | Full Grid All Edges Fixed |
| 2 | 13071001 | 10 | Full Grid All Edges Fixed |
| 2 | 14071000 | 10 | Full Grid, All Edges Fixed on Test Grid, Top Edge Fixed on Attached Grid |
| 2 | 21071000 | 10 | Full Grid, All Edges Fixed on Test Grid, Top Edge Fixed on Attached Grid |
| 2 | 21071001 | 8 | Full Grid, All Edges Fixed on Test Grid, Top Edge Fixed on Attached Grid |
| 2 | 21071002 | 6 | Full Grid, All Edges Fixed on Test Grid, Top Edge Fixed on Attached Grid |

3.2.1 Location 1

Location 1 was considered the least injurious location. Location 1 was on the longest free section of stainless steel rod, which essentially is a slender beam supported at two ends. The set up of the test is shown in Figure 9.

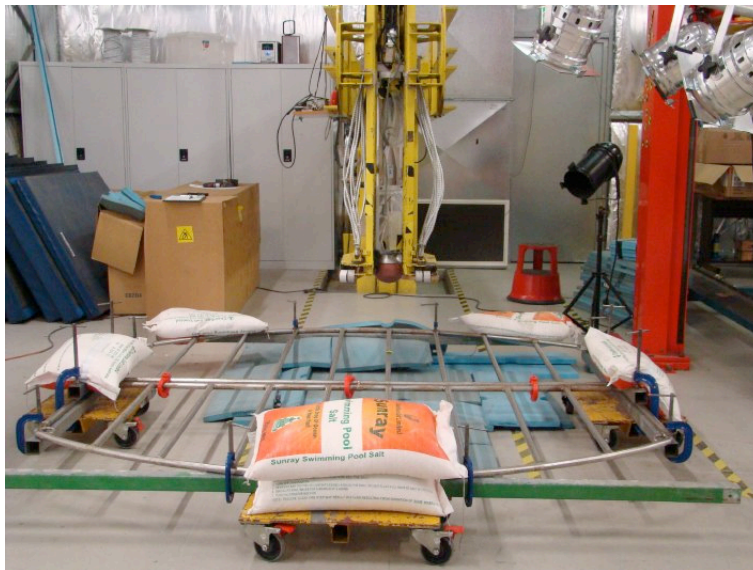


Figure 9
Set-up of the test for location 1 (test 13071000)

3.2.2 Location 2

Location 2 was assumed to be the most injurious location on the grid that would be easily accessible by a sea lion. Two boundary conditions were considered as shown in Figure 10. In the first set up (left), the top and side edges of each grid half were each clamped to the yellow platforms shown and the side edges of both grid halves were also clamped onto a steel beam so they were also restrained to each other. In the second configuration (right), the top edges of each grid half were clamped to the

yellow platforms, but only the side edges of the tested grid half were clamped onto the yellow platforms and steel beam. The side edges of the other half of the grid were not clamped to a platform and were allowed to rest on the steel beam without any clamping. The objective of this second test configuration was to simulate a slightly less rigid configuration and to evaluate the effect of this difference.

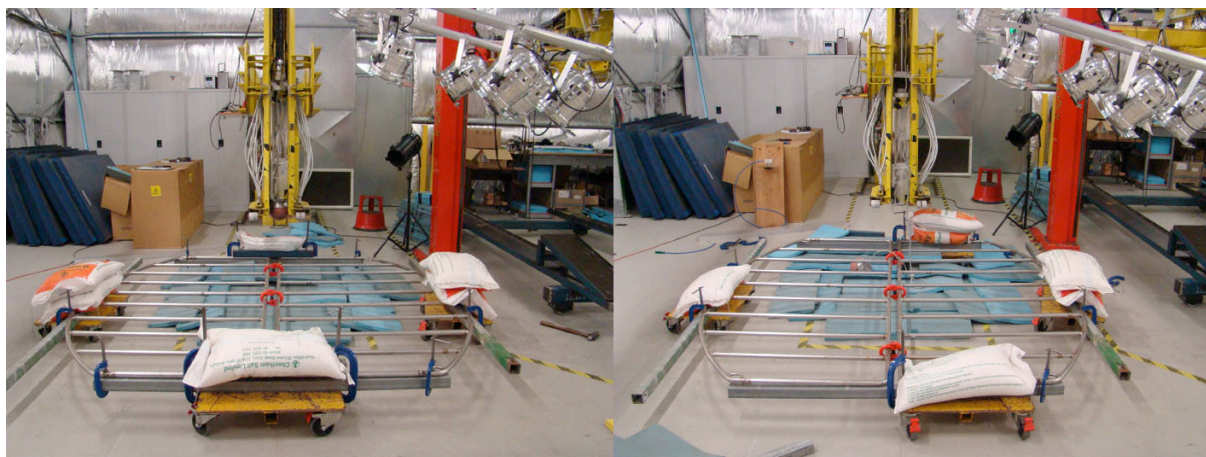


Figure 10

Set-up for location 2. The left set-up shows the top edges fixed and the side edges of both grid halves clamped to a steel beam (test 13071001). The right hand set-up shows the top edges fixed on each grid half, but only the tested grid half (on the right) fixed to the steel beam (test 14071000).

4 Results

4.1 Locations 1 and 2

The results from the test conducted at location 1 and 2 are show in Table 2.

Table 2
Test results for location 1 and 2

| Location | Test number | Impact Speed (m/s) | Peak acceleration (g) | HIC value | HIC window |
|----------|-------------|--------------------|-----------------------|-----------|------------|
| 1 | 13071000 | 10.08 | 345 | 1714 | 10.22 |
| 2 | 13071001 | 10.01 | 433 | 4003 | 2.8 |
| 2 | 14071000 | 10.14 | 439 | 3832 | 2.96 |
| 2 | 21071000 | 10.12 | 437 | 3580 | 2.96 |
| 2 | 21071001 | 8.21 | 336 | 2103 | 4.38 |
| 2 | 21071002 | 6.22 | 231 | 1047 | 4.36 |

The result of test 13071000 was generalised using Equation 1 with the objective of extending the result to other combinations of speed and mass. The effective mass of the sea lion head may be different from its dead weight. In an impact, forces may be transmitted through the neck from the rest of the body. Hence the head mass is effectively increased by the presence of these forces.

The upper panel in Figure 11 allows the result of the test to be scaled based on relative swim speeds and effective head masses. The lower graphs in Figure 11 show the corresponding injury risk curves for human tolerance, and that estimated for sea lion tolerance: an estimate based on a 1/3 power scaling relationship and an estimate based on a 2/3 power scaling relationship. These two graphs can be used in conjunction with different assumptions about the interactions between sea lions and the grid, and also different assumptions about impact tolerance, to assess the risk of injury. Table 6 (Appendix) presents these data in tabular form. The solid circular marker on the upper graph indicates the actual test result from which the curves are derived.

Consider, for example, a female sea lion with an effective head mass of 4.8 kg swimming at a relative speed of 10 m/s interacting with the SLED grid at location 1. This would result in a HIC of 1680. This corresponds to a risk of life-threatening brain injury of between 10% and 29%. The corresponding estimated risk of mild traumatic brain injury would be between 95% and 100%.

A total of three impact tests at the nominal impact speed of 10 m/s were conducted at location 2. The first impact test 13071001 resulted in a HIC of 4003 - the highest recorded for all the impacts. The second impact test at location 2 (test 14071000) resulted in a HIC of 3832. The third impact test at location 2 was conducted at a geometrically identical location under the same conditions as the second impact test at location 2, but on the other half of the grid. The resulting HIC was 3580. These differences in HIC between the three tests at location 2 indicate that alterations in the boundary conditions and slight structural differences have little effect on HIC.

Figure 12 relates the HIC values that might be generated from an impact with this location under varying impact conditions to the risk of head injury to the sea lion (based on the results from test 14071000). Table 7 presents the data in tabular form. The solid circular marker on the upper graph indicates the result of the actual test.

An interaction between a female adult sea lion with an effective head mass of 4.8 kg swimming at a relative speed 10 m/s and the SLED grid at location 2 would result in an estimated HIC of 3701. This corresponds to an estimated risk of life-threatening brain injury of between 85% and 100%. The corresponding estimated risk of mild traumatic brain injury is 100%.

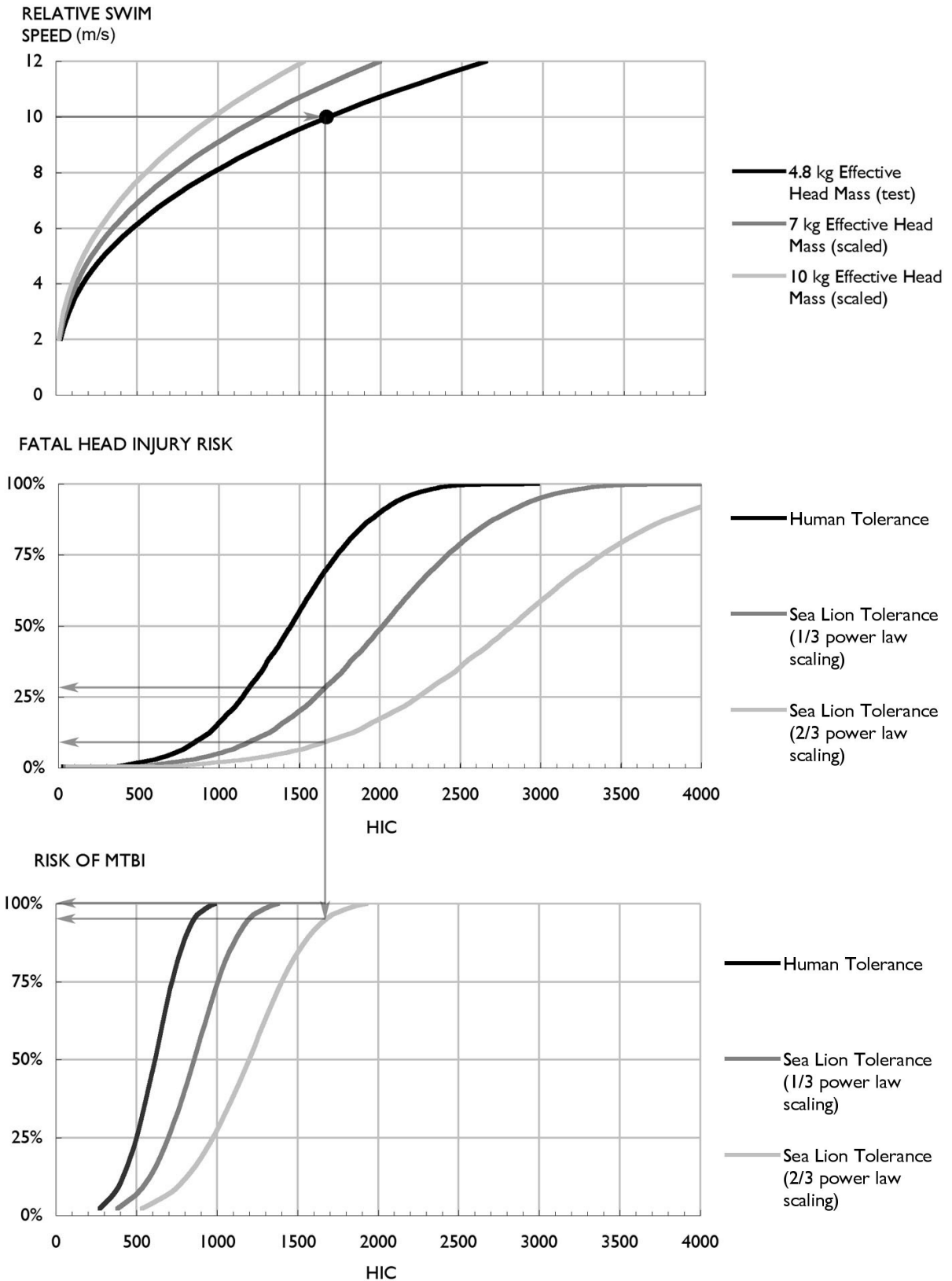


Figure 11

Results of the impact test at location 1 interpreted for alternative effective mass and swim speed assumptions and tolerance curves. Arrows refer to a relative swim speed of 10 m/s, an effective head impact mass of 4.8 kg, and estimates of fatal head injury risk as well as estimates of MTBI risk. The solid circular marker indicates the actual test result.

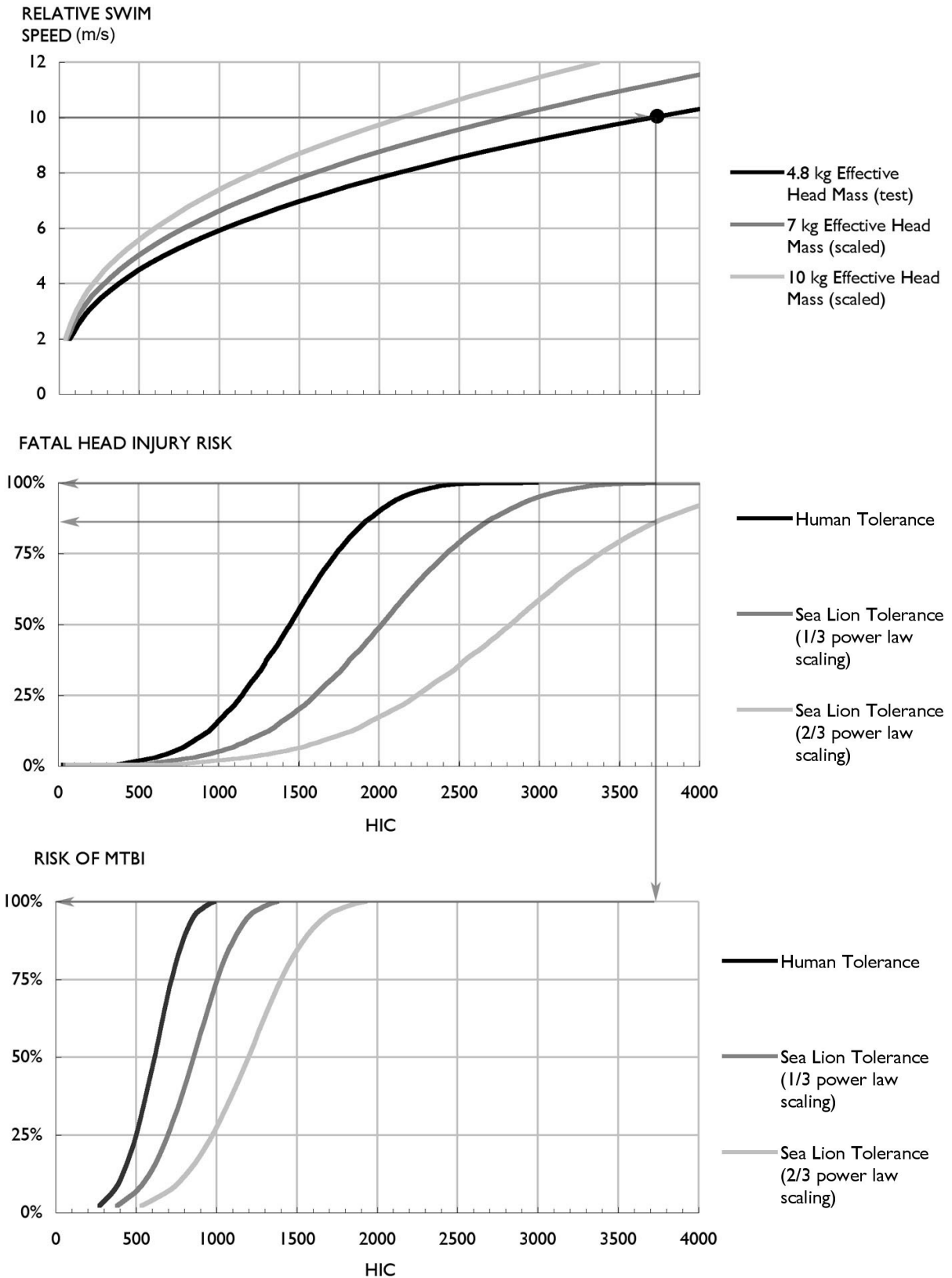


Figure 12

Results of the impact test at location 2 interpreted for alternative effective mass and swim speed assumptions and tolerance curves. Arrows refer to a relative swim speed of 10 m/s, an effective head impact mass of 4.8 kg, and estimates of fatal head injury risk as well as estimates of MTBI risk. The solid circular marker indicates the actual test result.

4.2 Location 3

Location 3 was investigated to examine the effect of different approach angles in impacts between a sea lion and the grid. Location 3 was on the horizontal mid bar. Figure 13 indicates how it might be possible for various approach angles to create different effective impact conditions, Figure 14 shows the experimental set-up for these tests.

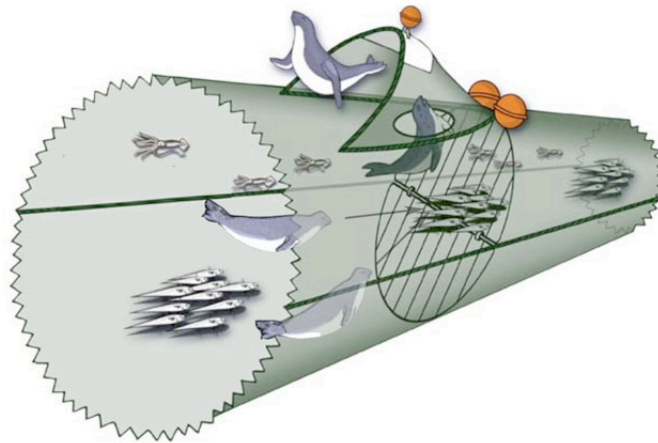


Figure 13

The SLED Grid demonstrating different possible angles of impact on the horizontal mid section of the grid (Adapted and modified from Tilzey and Wise, 2005)



Figure 14

Set-up for impact at location 3; impact angle 90, 60, 45 and 30 degrees respectively.

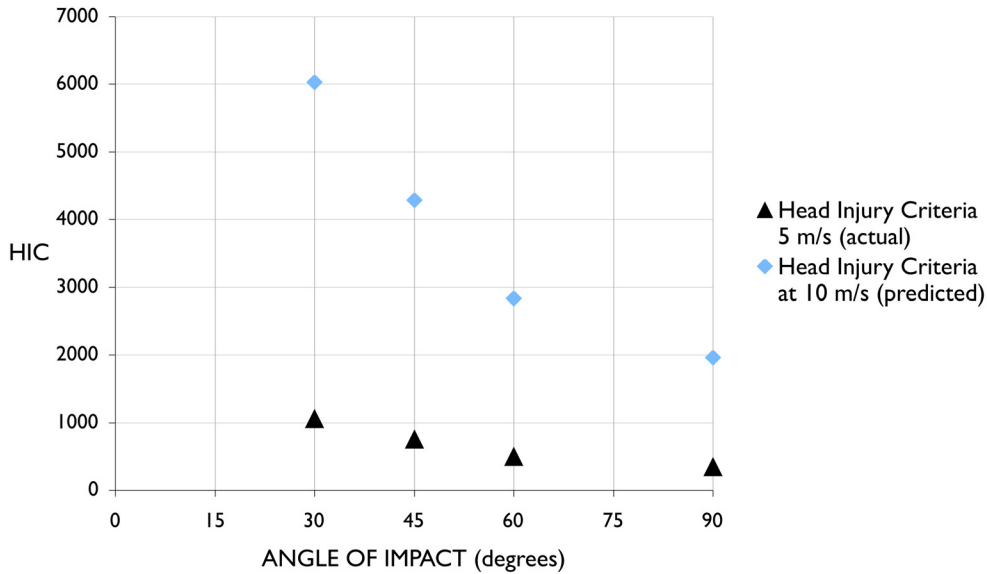


Figure 15
Impact angle and resulting Head Injury Criteria at location 3 (test speed 5 m/s)

As can be seen in Figure 15, there was a considerable increase in HIC as the angle of impact was decreased. At higher impact speeds (10 m/s) the differences in injury risk would be substantial. The effect is due to the geometrical construction of the grid. At an impact angle of 90 degrees, the grid is being restrained predominantly by the bending stiffness in the horizontal mid section bar and somewhat by bending stiffness of the shorter perpendicular bars. As the angle is increased, the perpendicular bars are increasingly put into tension (rather than bending). These bars are very stiff in tension and therefore the deflection of the horizontal bar is reduced, increasing impact forces.

4.3 Verification of scaling method

The two other impact tests at location 2, conducted at impact speeds of 8.21 m/s and 6.22 m/s, were used to verify the velocity component of the scaling equation (Equation 1). Table 3 shows the values of HIC resulting from or predicted for the various impact speeds. The speed shown in brackets indicates the speed used for the individual HIC prediction. Results were in good agreement with the scaling relationship used. That is, the HIC result from the test conducted at 8.21 m/s or 6.22 m/s, used in Equation 1 gives a good approximation of the HIC that was actually obtained in the test conducted at 10.14 m/s.

Table 3
Table showing the HIC values (actual and predicted) for the various test speeds.

| Speed (m/s) | 6.22 m/s | 8.21 m/s | 10.14 m/s |
|---|------------------|------------------|------------------|
| Test HIC | 1047 | 2103 | 3832 |
| Predicted HIC (speed of base test) | 1051 (8.21 m/s) | 2096 (6.22 m/s) | 3553 (6.22 m/s) |
| Predicted HIC (speed of base test) | 1129 (10.14 m/s) | 2260 (10.14 m/s) | 3565 (10.14 m/s) |

5 Discussion and Recommendations

The SLED grid we tested is a heavy and stiff structure. Its primary function is to divert sea lions and allow the targeted catch to filter through. The SLED was developed to reduce fishery-related mortality of sea lions, and is part of a strategy to contain fishery related mortality among New Zealand sea lions (New Zealand Ministry of Fisheries, 2010). However, the SLED's effectiveness remains in doubt. It is not known whether the SLED grid itself is a direct contributor to the mortality of the sea lions, but this report provides evidence suggesting that impacts with the grid in its current form may carry a risk of life threatening head injuries. At the location considered the stiffest, the SLED grid may cause life-threatening head injury at moderate to high swim speeds.

Even for lower speed impacts, where one might think that a sea lion interaction with the grid may not be very significant, the results of this study indicate that there is a risk of a sea lion suffering a mild traumatic brain injury. Although this impact may not be immediately fatal, it may have the potential to lead to death through drowning.

There are a number of uncertainties that limit the conclusiveness of these findings. We have assumed that sea lion interactions with SLEDs during trawling operations are resulting in head impacts with SLED grids. However, we could find only limited direct evidence for the nature of these interactions and we are aware of uncertainties in the interpretation of post-mortem findings in sea lion by-catch (Roe, 2010).

The purpose of this report was to document the probable injury risk that might occur from sea lion head impacts with the New Zealand SLED grid. Injury risks had to be inferred and are not known directly, but a reasoned estimate of injury risk has been presented, although it must be emphasised that the risks have been estimated only. Impact conditions are likewise not known and the effective mass of the head in interactions has been assumed to range between 4 and 10 kg. Given the stiffness of the grid, the duration of any impact will be short, and we therefore do not expect a large influence from the rest of the body on the impact.

Although the impact testing of the grid was not conducted underwater, it was assumed that this would have little effect on the impact characteristics of the grid. When the grid is submerged, the mass of the water acting on it during an impact would essentially be the mass of water directly behind each component of the grid, and given the small diameter of the components and the significant difference in density of the grid compared the water in which it is submerged, the effect of this mass would be small and can be ignored for the purpose of the analysis.

5.1 SLED grid design

The results from this report suggest that simple design changes might improve the outcome of an impact with certain parts of the grid.

According to the SLED Specification for SQU 6T 2010, the outside diameter should be constructed from 20 mm stainless steel bar (minimum) and bars should be spaced no more than 23 cm apart. The grid we tested was constructed from steel with a nominal diameter of 25 mm, spaced 23 cm apart. Each grid half weighed 56.5 kg. The equation for calculating the mass of a cylindrical rod per metre length h , for a particular radius r (in m), and density ρ (in kg/m^3) has a mass according to Equation 2.

$$\text{Mass}(\text{kg}/\text{m}) = \pi \times r^2 \times h \times \rho \quad \text{Equation 2}$$

$$Mass \propto r^2$$

Equation 3

Given that the mass of the rod is proportional to the square of the rod radius, as in Equation 3, a reduction in diameter of 25 mm to the minimum specification of 20 mm, would result in a mass decrease of 36%.

The mass is a significant factor in impact acceleration and corresponding HIC, and reductions in mass will lead to lower HIC. Additionally, the smaller diameter would lead to reduced stiffness, further reducing the HIC level.

The authors know little about the history of the design of the SLED grid. Obviously design constraints include strength and the minimisation of damage to catch. The bar spacing specifications (maximum 23 cm) are designed to “prevent 95% of the adult NZ sea lions measured, at their expected underwater diameter, from passing through the bars.” (Chilvers, 2005). Given this, some design changes to mitigate impact injury are suggested below in Figure 16.

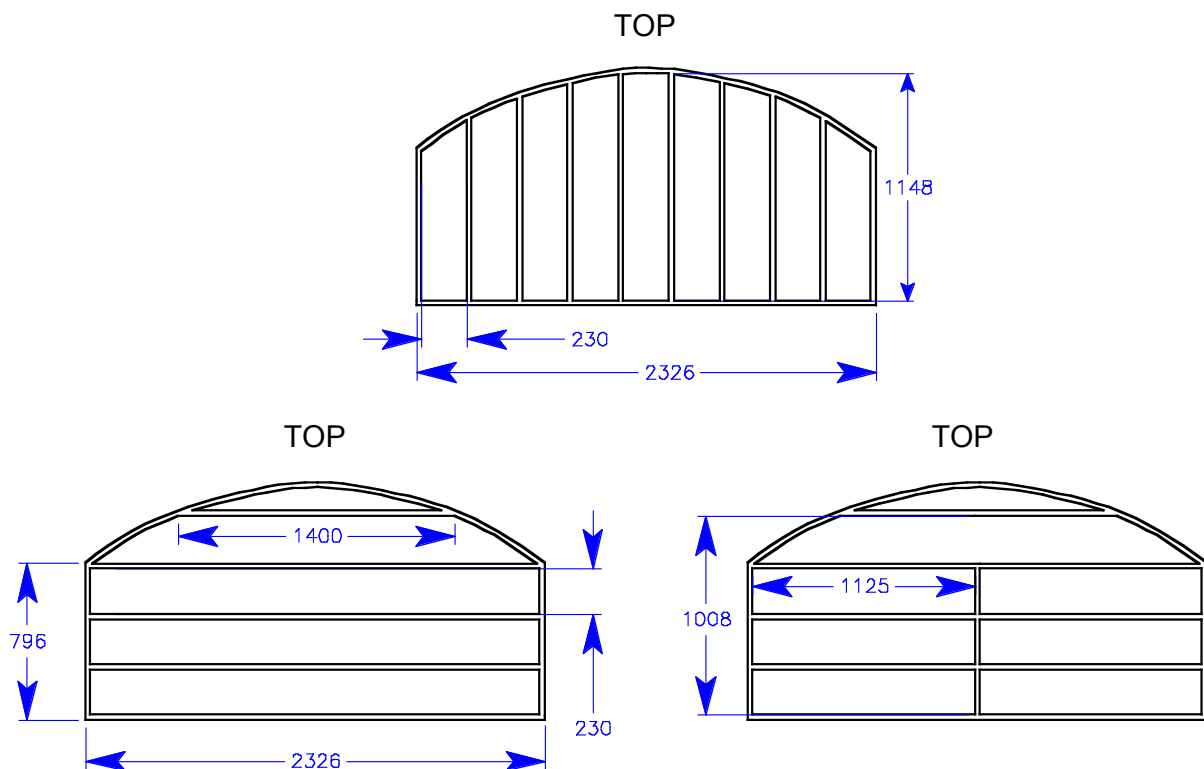


Figure 16

The tested SLED grid configuration (above) and suggested changes to SLED Grid design (below). Dimensions are in mm, and intended to be indicative

The SLED design shown in the top panel of Figure 16 is the design tested in this report. In the first alternative configuration shown (Figure 16, bottom left) the shortest rod length is around 1400 mm, slightly longer than the bar length tested in location 1 (around 1150 mm), which produced the lowest

risk of impact injury. The stiff locations in this configuration are restricted to the outer edge intersections of the grid half and are eliminated from the horizontal mid section. This grid design has around the same total length of rod as in the original design, and therefore similar mass in the 25 mm diameter rod configuration. A concern that may arise with this grid design is that the length of the bars may be too long and might cause sea lions to wedge between the bars if they have too much vertical flexion. The simple solution is the second design (Figure 16, right), which includes an additional vertical support across the centre of the grid to reduce flexion, and need not be to the same specification as the rest of the grid (i.e. can be smaller diameter, less rigid, just to tie the rod lengths together).

One alternative to a SLED grid constructed from stainless steel rod might be a polyethylene blow moulded grid, similar to the polyethylene bull bars offered as alternative to steel and alloy bull bars on vehicles. These plastic bull bars lower HIC results considerably compared to metal bull bars (Anderson et al, 2006). Any changes that reduce the stiffness of the grid itself and the rigidity in the way it is attached to the trawl net will result in lower impact severity.

Another alternative might be a net of some sort, constructed from thick cord, with of grid size of about 180 mm x 180 mm or 220 mm x 220 mm. Such a net would allow the required catch to filter through and divert sea lions without causing significant impact injuries. Even if the outer diameter of the current grid design were retained, but with net replacing the vertical bars, then the number of locations carrying a high risk of impact injury would be reduced.

6 Acknowledgements

This study was funded by the New Zealand Ministry of Fisheries.

The authors wish to acknowledge the support of Dr Eric Mellina and Dr Martin Cryer, Aquatic Environment, Ministry of Fisheries and Dr Wendi Roe, Massey University New Zealand.

The authors would also like acknowledge the support of Carolyn Collier from Hampidjan NZ Ltd, Timaru, New Zealand who generously provided the SLED grid for testing.

The views expressed in this report are those of the authors and do not necessarily represent those of the University of Adelaide or the NZ Ministry of Fisheries.

7 References

Anderson RWG, van den Berg AL, Ponte G, Streeter LD, McLean AJ (2006) Performance of bull bars pedestrian impact tests (CASR020). Adelaide: Centre for Automotive Safety Research.

Chilvers BL (2005). Female New Zealand sea lion body size and SLED specifications. Report to the Ministry of Fisheries SLED Working Group, 15 June 2005 (Unpublished report held by Ministry of Fisheries, Wellington), as cited in:

New Zealand Department of Conservation, Development of a Prototype fur seal exclusion device (SED). New Zealand, viewed 4 August 2010 <http://www.doc.govt.nz/upload/documents/conservation/marine-and-coastal/fishing/twg/fur-seal-mitigation-draft-excl-device-proposal.pdf>

DWG and MFish (2009) SLED Specification for SQU 6T 2010 Operational Plan.

Fish, Frank. 2002. pp. 1161-1163. Encyclopedia of Marine Mammals, Perrin Editor, Academic Press

Funk JR, Duma SM, Manoogian SJ, Rowson S (2007) Biomechanical risk estimates for mild traumatic brain injury. Proceedings of the 51st Annual Scientific Conference for the Association for the Advancement of Automotive Medicine, Melbourne, Australia.

Gennarelli TA, Thibault LE, Adams JH, Graham DI, Thompson CJ, Marcincin RP (1982) Diffuse axonal injury and traumatic coma in the primate, *Annals of Neurology*, 12(6), pp 564-574.

Goldsmith W, Plunkett J (2004) A Biomechanical Analysis of the Causes of Traumatic Brain Injury in Infants and Children. *The American Journal of Forensic Medicine and Pathology*; Vol 25(2), pp 89-100.

Lyle JM, Willcox ST (2008) Dolphin and seal interactions with mid-water trawling in the Commonwealth small pelagic fishery, including and assessment of by catch mitigation (Report R05/0996). Canberra: Australian Fisheries Management Authority.

Mertz H J (1993). Anthropomorphic test devices. In (Eds Nahum AM and Melvin JW) *Accidental Injury - Biomechanics and Prevention*. New York: Springer-Verlag. pp 66-84., as cited in:

Lawrence GJL, with contributions from EEVC WG17 members (2005). The next steps for pedestrian protection test methods. Proceedings of 19th ESV Conference 2005, Washington D.C.

New Zealand Ministry of Fisheries (2010) Arrow Squid, viewed on August 2010 <http://fs.fish.govt.nz/Page.aspx?pk=113&dk=22257>

Ommaya AK, Yarnell P, Hirsch AE, Harris E (1967) Scaling of experimental data on cerebral concussion in sub-human primates to concussion threshold for man. Proceedings of the 11th Stapp Car Crash Conference, New York: Society of Automotive Engineers, pp 47-52.

Ray, G. C. (1963). Locomotion in pinnipeds. *Natural History* 72: 10 -21

Roe, W. 2010. External review of NZ sea lion bycatch necropsy data and methods. Available from Aquatic Sciences, [The](#) New Zealand Ministry of Fisheries, Box 1020, Wellington, New Zealand.

Searson DJ, Anderson RWG (2008) Pedestrian Impact Testing: Modelling the Effect of Head-form Mass and Speed, Proceedings of 2008 Australasian Road Safety Research, Policing and Education Conference. Adelaide: Department for Transport, Energy and Infrastructure, pp 23-32.

Tilzey R, Wise B (2005) Seal of Approval - Do Seal Exclusion Devices Work? Australian Government Bureau of Rural Sciences Seminar, Canberra, 25 February 2005.

8 Appendices

Table 4

The raw data used to generate the risk curves for fatal head injury, derived from Mertz (1993) and the corresponding predicted HIC for Sea Lion fatal head injury.

| Risk of Fatal Head Injury | HIC in humans | Sea Lion HIC based on a 1/3 power law relationship with brain mass | Sea Lion HIC based on a 2/3 power law relationship with brain mass |
|---------------------------|---------------|--|--|
| 0% | 30 | 42 | 59 |
| 0% | 182 | 254 | 354 |
| 0% | 273 | 381 | 531 |
| 0% | 364 | 507 | 708 |
| 2% | 538 | 751 | 1048 |
| 3% | 613 | 856 | 1195 |
| 3% | 614 | 856 | 1195 |
| 4% | 650 | 907 | 1266 |
| 5% | 704 | 982 | 1371 |
| 5% | 704 | 983 | 1372 |
| 7% | 778 | 1086 | 1516 |
| 7% | 779 | 1087 | 1516 |
| 9% | 856 | 1195 | 1667 |
| 9% | 856 | 1195 | 1667 |
| 13% | 947 | 1322 | 1844 |
| 16% | 1000 | 1396 | 1948 |
| 17% | 1023 | 1427 | 1992 |
| 22% | 1114 | 1554 | 2169 |
| 26% | 1159 | 1618 | 2257 |
| 29% | 1205 | 1681 | 2346 |
| 34% | 1265 | 1766 | 2464 |
| 38% | 1311 | 1829 | 2553 |
| 42% | 1356 | 1893 | 2641 |
| 47% | 1417 | 1977 | 2759 |
| 51% | 1462 | 2040 | 2848 |
| 56% | 1508 | 2104 | 2936 |
| 63% | 1583 | 2210 | 3084 |
| 68% | 1644 | 2294 | 3202 |
| 71% | 1689 | 2358 | 3290 |
| 75% | 1735 | 2421 | 3379 |
| 80% | 1811 | 2527 | 3526 |
| 86% | 1902 | 2654 | 3703 |
| 89% | 1977 | 2759 | 3851 |
| 93% | 2068 | 2886 | 4028 |
| 95% | 2152 | 3003 | 4190 |
| 98% | 2294 | 3201 | 4467 |
| 100% | 2480 | 3461 | 4830 |
| 100% | 2985 | 4165 | 5813 |

Table 5

The raw corrected data used to generate the risk curves for mild traumatic brain injury (MTBI), derived from Funk et al (2007) and the corresponding predicted HIC for Sea Lion MTBI.

| Risk of Mild Traumatic Brain Injury | HIC in humans | Sea Lion HIC based on a 1/3 power law relationship with brain mass | Sea Lion HIC based on a 2/3 power law relationship with brain mass |
|-------------------------------------|---------------|--|--|
| 2% | 274 | 382 | 533 |
| 8% | 370 | 516 | 720 |
| 14% | 432 | 602 | 840 |
| 23% | 494 | 689 | 961 |
| 36% | 556 | 775 | 1082 |
| 50% | 618 | 862 | 1203 |
| 66% | 680 | 948 | 1324 |
| 79% | 742 | 1035 | 1444 |
| 89% | 804 | 1122 | 1565 |
| 95% | 866 | 1208 | 1686 |
| 98% | 928 | 1295 | 1807 |
| 100% | 990 | 1381 | 1927 |

Table 6

Scaled and tabulated HIC values from the impact test at location 1.

| Effective Head Mass (kg) | Relative Swim Speed (m/s) | | | | | | | | | |
|--------------------------|---------------------------|----|-----|-----|-----|-----|------|------|------|------|
| | 2 | 3 | 4 | 5 | 6 | 7 | 8 | 9 | 10 | 11 |
| 4 | 34 | 95 | 195 | 341 | 537 | 790 | 1103 | 1480 | 1926 | 2445 |
| 4.8 | 30 | 83 | 170 | 297 | 469 | 689 | 962 | 1291 | 1680 | 2132 |
| 5 | 29 | 80 | 165 | 288 | 454 | 668 | 933 | 1252 | 1630 | 2068 |
| 6 | 25 | 70 | 144 | 251 | 396 | 583 | 814 | 1092 | 1421 | 1804 |
| 7 | 23 | 62 | 128 | 224 | 353 | 519 | 725 | 973 | 1266 | 1607 |
| 8 | 20 | 56 | 116 | 202 | 319 | 470 | 656 | 880 | 1145 | 1454 |
| 9 | 19 | 52 | 106 | 185 | 292 | 430 | 600 | 806 | 1049 | 1331 |
| 10 | 17 | 48 | 98 | 171 | 270 | 397 | 555 | 745 | 969 | 1230 |
| 11 | 16 | 44 | 91 | 159 | 252 | 370 | 516 | 693 | 902 | 1145 |

Table 7

Scaled and tabulated HIC values from the impact at location 2.

| Effective Head Mass (kg) | Relative Swim Speed (m/s) | | | | | | | | | |
|--------------------------|---------------------------|-----|-----|-----|------|------|------|------|------|------|
| | 2 | 3 | 4 | 5 | 6 | 7 | 8 | 9 | 10 | 11 |
| 4 | 76 | 209 | 429 | 750 | 1183 | 1740 | 2429 | 3261 | 4243 | 5385 |
| 4.8 | 66 | 182 | 375 | 654 | 1032 | 1517 | 2119 | 2844 | 3701 | 4697 |
| 5 | 64 | 177 | 363 | 635 | 1001 | 1472 | 2055 | 2758 | 3590 | 4555 |
| 6 | 56 | 154 | 317 | 553 | 873 | 1283 | 1792 | 2406 | 3131 | 3973 |
| 7 | 50 | 137 | 282 | 493 | 778 | 1143 | 1596 | 2143 | 2789 | 3539 |
| 8 | 45 | 124 | 255 | 446 | 704 | 1034 | 1444 | 1939 | 2523 | 3202 |
| 9 | 41 | 114 | 234 | 408 | 644 | 947 | 1322 | 1775 | 2310 | 2931 |
| 10 | 38 | 105 | 216 | 377 | 595 | 875 | 1222 | 1640 | 2134 | 2709 |
| 11 | 36 | 98 | 201 | 351 | 554 | 815 | 1137 | 1527 | 1987 | 2522 |

Table 8 Generic table of alphanumerics and corresponding equation for linear interpolation.

| | |
|----------|----------|
| <i>X</i> | <i>A</i> |
| <i>Y</i> | <i>B</i> |
| <i>Z</i> | <i>C</i> |

$$B = A + (Y - X) \left(\frac{C - A}{Z - X} \right) \quad (2)$$